Dyes and Pigments 91 (2011) 404–412

Contents lists available at ScienceDirect

Dyes and Pigments

journal homepage: www.elsevier.com/locate/dyepig

Multi-alkylthienyl appended porphyrins for efficient dye-sensitized solar cells

Weiping Zhou [a], Bin Zhao [a,b], Ping Shen [a,b], Shenghui Jiang [a], Hongduan Huang [a], Lijun Deng [a], Songting Tan [a,b,*]

[a] College of Chemistry, Key Laboratory of Environmentally Friendly Chemistry and Applications of Ministry of Education, Xiangtan University, Xiangtan 411105, PR China
[b] Key Laboratory of Advanced Functional Polymeric Materials, College of Hunan Province, Xiangtan University, Xiangtan 411105, PR China

ARTICLE INFO

Article history:
Received 1 February 2011
Received in revised form
15 May 2011
Accepted 16 May 2011
Available online 2 June 2011

Keywords:
Multi-alkylthienyl porphyrins
Thiophene derivatives
Red-shifted
Power conversion efficiency
Dye-sensitized solar cells
Photovoltaic performance

ABSTRACT

Four porphyrin dyes, incorporating multi-alkylthienyl appended porphyrins as the electron donor, the 2-cyanoacrylic acid as the electron acceptor, and different π-conjugated spacer, have been synthesized for dye-sensitized solar cells (DSSCs). All the porphyrin dyes studied in this work exhibit red-shifted and broadened electronic spectra respect to the reference $\mathbf{P_{Zn}}$ as expected. By the introduction of thienyl groups at the *meso*-positions, the energy level of E_{ox} (excited-state oxidation potentials) is significantly shifted to the positive compared with the reference $\mathbf{P_{Zn}}$, indicating a decreased HOMO–LUMO gap. The highest power conversion efficiency of the four dyes based on DSSCs reached 5.71% under AM 1.5 G irradiation.

1. Introduction

Increasing energy demand pushes human beings to find more and more renewable energy sources. Solar energy plays a key role as a renewable, clean and inexhaustible resource [1]. From the breakthrough by Grätzel and co-workers [2], the research on dye-sensitized solar cells (DSSCs) has intensified in recent years [3,4]. Nowadays, DSSCs based on the ruthenium sensitizers have achieved power conversion efficiencies (η) of 10–11% [5]. However, ruthenium dyes are expensive due to the cost of ruthenium and the typically lengthy purification steps involved in their preparation. Alternative low cost and readily accessible ruthenium dye replacements are under active investigation. Porphyrins are one of the alternative dyes used as sensitizers with many advantages as follows. 1) The porphyrins derived from chlorophylls which are the key components of natural photosynthetic systems in green plants [6] and absorb strongly in the range of 400–700 nm with high molar absorbance coefficient. 2) Porphyrin dyes have been demonstrated to possess charge-transfer kinetics indistinguishable from those of ruthenium polypyridyl complexes [7]. 3) Metal porphyrins undergo facile reduction and oxidation [8], so their optical, photophysical, and electrochemical properties can be systematically tailored by the peripheral substitutions and/or inner metal complexations. Porphyrins, however, generally show inferior performance due to the limited light absorption, poor matching to solar light distribution, and consequently possess a low value of short circuit current. To achieve higher η, two methods have been studied: elongating the π-system and lowering the symmetry of the macro-cycle [8], which can lead to a significantly broadened Soret-band and a red-shifted Q-band absorptions. A DSSC device using porphyrin sensitizers with the linker and anchor units functionalized at the β-position is reported to show a η as high as 7.1% [9]. Diau et al. synthesized a series of dark-green porphyrin sensitizers with phenylethylnyl as linkers and carboxyl groups as anchors at the *meso*-position with the η in the range from 2.1% to 11% in DSSCs [10].

In recent years, interest in *meso*-tetrathienylporphyrins is growing due to their use as models for energy transfer reactions [11]. In almost all porphyrin structures applied in DSSCs, the substituents at the *meso*-positions are phenyl units. However, the smaller five-membered 2-thienyl rings offer reduced steric hindrance compared with the larger six-membered 4-phenyl rings. In addition, the 2-thienyl group lacks one *o*-phenyl-H to β-pyrrole-H interaction which allows for greater easy of rotation of the

* Corresponding author. College of Chemistry, Key Laboratory of Environmentally Friendly Chemistry and Applications of Ministry of Education, Xiangtan University, Xiangtan 411105, PR China.
E-mail address: tanst2008@163.com (S. Tan).

0143-7208/$ – see front matter © 2011 Elsevier Ltd. All rights reserved.
doi:10.1016/j.dyepig.2011.05.017

thien-2-yl porphyrins, thus allowing the thienyl groups to adopt a coplanar arrangement to the porphyrin ring [12]. Moreover, it is known that the attachment of thienyl units usually can induce a bathochromic shift, an intensification of the absorptivity and an increased lifetime of the excited-state [13]. Until now, there are few investigations of *meso*-tetrathienylporphyrins applied in DSSCs. In this study, we designed and synthesized a series of multi-thienyl appended porphyrin dyes (**Z1**–**Z4**) with D–π–A structure (see Fig. 1) applied in DSSCs. For comparison, the structure of the reference porphyrin dye $\mathbf{P_{Zn}}$ is also shown in Fig. 1. The thiophene segments with varied substituents employed as bridges (π) for linking the porphyrin donors (D) and anchoring and acceptor groups (A), as well as extending the π-conjugated bridges. Three 5-alkylthien-2-yl groups are introduced to improve the electronic spectra and to tune the redox potential. Further, the alkyl groups can induce steric hindrance around the porphyrin core to reduce the aggregation between the neighboring porphyrins adsorbed onto the TiO_2 surface.

2. Experimental section

2.1. Materials and reagents

All starting materials were purchased from commercial suppliers (Pacific ChemSource and Alfa Aesar Corp.) at analytical grade. THF and toluene were distilled from sodium–benzophenone prior to use. DMF was dried and distilled under reduced pressure. $POCl_3$ and 1,2-dichloroethane were achieved by atmospheric distillation. All other solvents and chemicals used in this work were analytical grade without further purification. All chromatographic separations were carried out on silica gel (200–300 mesh).

2.2. Analytical instruments

FT-IR spectra were measured on a Perkin–Elmer Spectra One spectrophotometer. ^1H and ^{13}C NMR spectra were recorded with a Bruker Avance 400 instrument. UV–visible spectra of the dyes were measured on a Perkin–Elmer Lambda 25 spectrophotometer. The PL spectra were obtained using Perkin–Elmer LS-50 luminescence spectrophotometer. MALDI–TOF mass spectrometric measurements were performed on Bruker Autoflex III. Electrochemical redox potentials were obtained by cyclic voltammetry (CV) and differential pulse voltammetry (DPV) using a three-electrode configuration and an electrochemistry workstation (CHI660A, Chenhua Shanghai). The working electrode was a glassy carbon electrode; the counter electrode was a Pt electrode, and saturated calomel electrode (SCE) was used as a reference electrode. Tetrabutylammonium perchlorate (TBAP) 0.1 M was used as the supporting electrolyte in dry DMF. Ferrocene was added to each sample solution at the end of the experiments, and was used as an internal potential reference [14].

2.3. General procedure for preparation of porphyrin-modified TiO_2 electrode and photovoltaic measurements

The TiO_2 suspension was prepared from P25 (Degussa AG, Germany) and 1 wt% magnesium acetate solution on following a literature procedure [15]. The suspension was deposited on a transparent conducting glass by using a doctor blade technique. The film was sintered at 450 °C for 30 min, then treated with 40 mM $TiCl_4$ aqueous solution at 70 °C for 30 min and annealed again at 450 °C for 30 min. After the film was cooled to room temperature, it was immersed into 5.0×10^{-4} M dye solution for 15 min in the dark. The sensitized electrode was then rinsed with ethanol, and dried. One drop of electrolyte solution was deposited onto the surface of the electrode and penetrated inside the TiO_2 film via capillary action. The photovoltaic measurements were performed in a sandwich cell consisting of the porphyrin-sensitized TiO_2 electrode as the working electrode and a Pt foil as the counter electrode. The electrolyte consists of 0.5 M LiI, 0.05 M I_2, and 0.5 M 4-*tert*-butylpyridine (TBP) in 3-methoxypropionitrile. The photocurrent-voltage (*J*–*V*) characteristics were recorded on Keithley 2602 Source meter. Porphyrin dyes sensitized TiO_2 electrodes were measured under simulated AM 1.5 irradiation

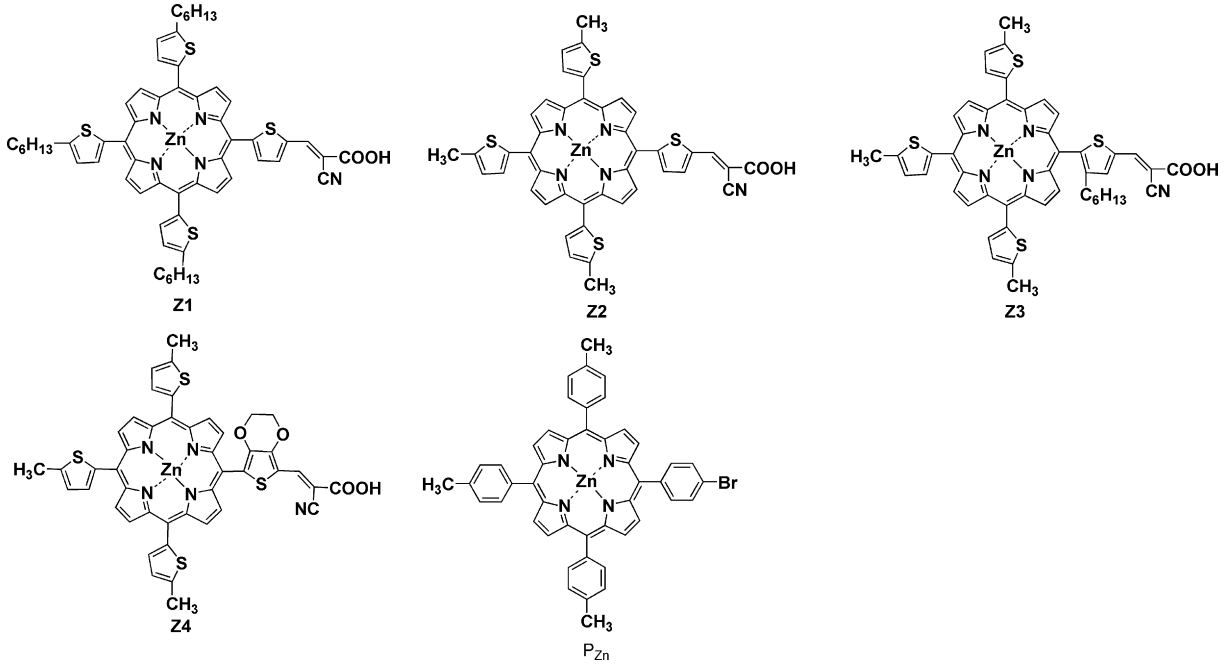

Fig. 1. Molecular structures of the porphyrin dyes **Z1**–**Z4** and $\mathbf{P_{Zn}}$.

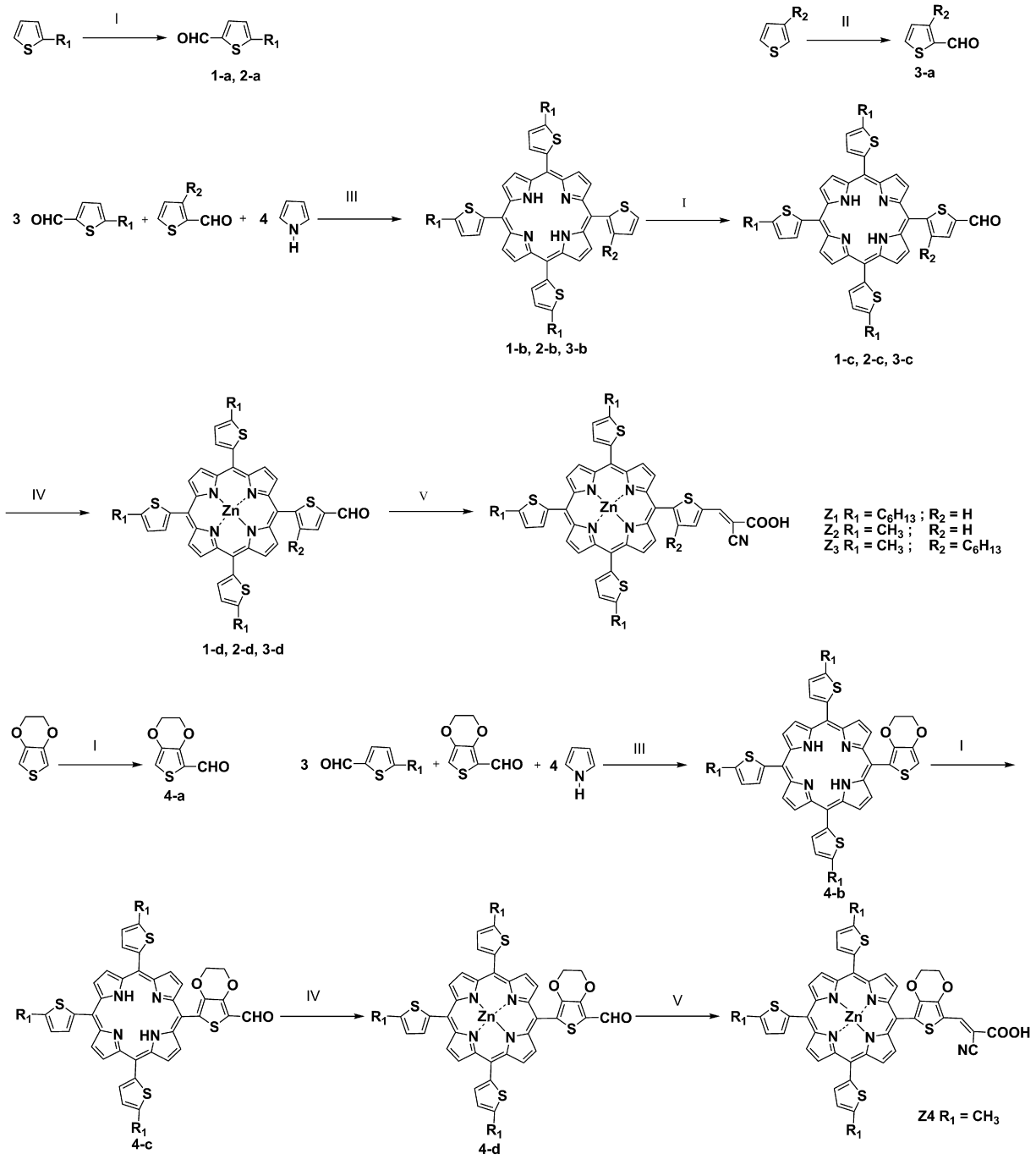

Fig. 2. Synthetic routes to the porphyrin dyes. Reagents and conditions: I, $POCl_3$, DMF, 1,2-dichloroethane; II, Mg, I_2, THF, DMF; III, propionic acid; IV, $Zn(OAc)_2$, CH_3OH, $CHCl_3$; V, cyanoacetic acid, piperidine, CH_3CN.

(100 mW cm^{-2}). The power conversion efficiency (η) of the DSSCs is calculated from short-circuit photocurrent (J_{sc}), the open-circuit photovoltage (V_{oc}), the fill factor (ff) and the intensity of the incident light (P_{in}) according to the following equation:

$$\eta = \frac{J_{sc}\left(\text{mA cm}^{-2}\right) \times V_{oc}(V) \times ff}{P_{in}\left(\text{mW cm}^{-2}\right)}$$

The incident photon-to-current conversion efficiency (IPCE) values are plotted as a function of the excited wavelength and defined according to the following equation [16]:

$$\text{IPCE}(\lambda) = \frac{1240}{\lambda(\text{nm})} \times \frac{J_{sc}\left(\text{mA cm}^{-2}\right)}{\Phi\left(\text{mW cm}^{-2}\right)}$$

Where J_{sc} is the short-circuit photocurrent density generated by monochromatic light, λ is the wavelength of incident monochromatic light, and Φ is the incident light intensity.

2.4. Synthesis

5-Hexylthiophene-2-carbaldehyde (**1-a**), 5-methylthiophene-2-carbaldehyde (**2-a**), 3,4-ethylenedioxylthienyl-2-carbaldehyde (**4-a**),

were synthesized according to the methods reported in the literature [17] with some modification. The synthetic routes to the four dyes are shown in Fig. 2. The detailed synthetic procedures are as follows.

*2.4.1. 5-(Thien-2-yl)-10,15,20-tris(5-hexylthien-2-yl)porphyrin (**1-b**)*

In a 250 mL three-necked round-bottomed flask, 5-hexyl thiophene-2-carbaldehyde (**1-a**) (7.2 g, 36 mmol), thiophene-2-carbaldeyde (1.37 g, 12 mmol) were dissolved in propionic acid (200 mL) and the solution was heated under reflux at 140 °C.Pyrrole (3.21 g, 48 mmol) was added dropwise and stirred for another 30 min. After cooling to room temperature, the solvent was evaporated and the crude product was separated by column chromatography (petroleum ether/dichloromethane = 3/1 as an eluent). After recrystallization from CH_3OH, the desired bright purple solid compound **1-b** was obtained (1.2 g, 11.2%). ^{1}H NMR ($CDCl_3$, 400 MHz, δ/ppm): 9.09–9.02 (*d*, 8 H, pyrrolic-H), 7.91 (*d*, 1 H, Th–H), 7.86–7.84 (*d*, 1 H, Th–H), 7.69 (*d*, 3 H, Th–H), 7.50 (*d*, 1 H, Th–H), 7.17 (*d*, 3 H, Th–H), 3.15–3.11 (*t*, 6 H, $-CH_2$), 1.99–1.92 (*m*, 6 H, $-CH_2$), 1.61–1.58 (*m*, 6 H, $-CH_2$), 1.45 (*m*, 12 H, $-CH_2$), 0.99–0.96 (*t*, 9 H, $-CH_3$), −2.61 (*s*, 2 H, −NH). ^{13}C NMR ($CDCl_3$, 100 MHz, δ/ppm):148.9, 140.1, 140.0, 133.8, 133.6, 131.1, 127.8, 126.0, 123.3, 113.0, 112.9, 31.9, 31.7, 30.4, 29.0, 22.7, 14.1. MALDI–TOF MS ($C_{54}H_{58}N_4S_4$) *m*/*z*: calcd for 891.33; found 891.57.

*2.4.2. 5-(5-Formylthien-2-yl)-10,15,20-tris(5-hexylthien-2-yl) porphyrin (**1-c**)*

In a 50 mL three-necked flask, porphyrin **1-b** (0.53 g, 1 mmol), DMF (1 mL, 12 mmol), 1,2-dichloroethane (15 mL) were added sequentially under Ar atmosphere. $POCl_3$ (1.1 mL, 12 mmol) was added quickly at 0 °C. The mixture was heated to 80 °C and stirred for 12 h. After cooling to room temperature, poured it into sodium acetate solution and stirred for an addition 1 h. The solution was extracted with dichloromethane, and washed with H_2O and brine. The organic layer was dried over anhydrous $MgSO_4$. Solvent was removed by rotary evaporation, and the residue was purified by silica gel column chromatography with petroleum ether/dichloromethane (1/1) as eluent to yield **1-c** as a purple-red solid (0.22 g, 40%). ^{1}H NMR ($CDCl_3$, 400 MHz, δ/ppm): 10.26 (*s*, 1 H, −CHO), 9.11–8.97 (*m*, 8 H, pyrrolic-H), 8.16–8.15 (*d*, 1 H, Th–H), 8.00–7.99 (*d*, 1 H, Th–H), 7.71–7.70 (*d*, 3 H, Th–H), 7.18–7.17 (*d*, 3 H, Th–H), 3.15–3.11 (*t*, 6 H, $-CH_2$), 1.99–1.92 (*m*, 6 H, $-CH_2$), 1.62–1.57 (*m*, 6 H, $-CH_2$), 1.44(*m*, 12 H, $-CH_2$), 0.99–0.96 (*m*, 9 H, $-CH_3$), −2.61 (*s*, 2 H, −NH). ^{13}C NMR ($CDCl_3$, 100 MHz, δ/ppm):183.2, 153.4, 149.1, 145.7, 139.8, 134.7, 133.8, 123.3, 113.5, 109.7, 31.8, 31.7, 30.4, 29.0, 22.6, 14.1. MALDI–TOF MS ($C_{55}H_{58}N_4OS_4$) *m*/*z*: calcd for 919.32; found 919.34.

*2.4.3. 5-(5-Formylthien-2-yl)-10,15,20-tris(5-hexylthien-2-yl) porphyrin zinc (**1-d**)*

A mixture of compound **1-c** (0.55 g, 1 mmol) and Zn $(OAc)_2$ (1.85 g, 10 mmol) in $CHCl_3$ (150 mL) and CH_3OH (10 mL) was refluxed for 4 h. After cooling to room temperature, the mixture was washed with H_2O. The organic layer was dried over anhydrous $MgSO_4$ and concentrated by rotary evaporation. A purplish-green solid of compound **1-d** was obtained (0.55 g, 95%). ^{1}H NMR ($CDCl_3$, 400 MHz, δ/ppm): 10.26 (*s*, 1 H, −CHO), 9.12–8.98 (*m*, 8 H, pyrrolic-H), 8.15 (*d*, 1 H, Th–H), 7.99 (*d*, 1 H, Th–H), 7.70 (*d*, 3 H, Th–H), 7.17 (*d*, 3 H, Th–H), 3.15–3.11 (*t*, 6 H, $-CH_2$), 1.99–1.92 (*m*, 6 H, $-CH_2$), 1.62–1.57 (*m*, 6 H, $-CH_2$), 1.44 (*m*, 12 H, $-CH_2$), 0.99–0.96 (*m*, 9 H, $-CH_3$). MALDI–TOF MS ($C_{55}H_{56}N_4OS_4Zn$) *m*/*z*: calcd for 981.24; found 981.33.

2.4.4. 2-Cyano-3-(5-(10,15,20-tris(5-hexylthien-2-yl)) porphyrinatozinc(II)yl)thienyl acrylic acid (Z1)

To a solution of acetonitrile (15 mL) and toluene (5 mL), porphyrin compound **1-d** (0.180 g, 0.29 mmol), cyanoacetic acid (0.073 g, 0.87 mmol) and piperidine (0.5 mL) were added sequentially under Ar atmosphere, the mixture was heated under reflux for 16 h. After cooling to room temperature, the solution was extracted with dichloromethane, and washed with H_2O and 0.1 M HCl. The organic layer was dried over anhydrous $MgSO_4$. Solvent was removed by rotary evaporation, and the residue was purified by silica gel column chromatography with methanol/dichloromethane (1/20) as eluent to yield a purple solid **Z1** (0.11 g, 57%). FT-IR (KBr, ν_{max}/cm^{-1}): 2977, 2927, 2347, 2219, 1651, 1488, 1400, 1068, 989, 794, 703, 666. UV–vis λ_{max} ($CHCl_3$)/nm: 434, 559. ^{1}H NMR (DMSO, 400 MHz, δ/ppm): 9.06–9.00 (*m*, 8 H, pyrrolic-H), 8.58 (s, 1 H, vinyl-H), 8.31 (*s*, 1 H, Th–H), 8.11 (*s*, 1 H, Th–H), 7.74 (*d*, 3 H, Th–H), 7.28 (*d*, 3 H, Th–H), 3.12 (*t*, 6 H, $-CH_2$), 1.89 (*t*, 6 H, $-CH_2$), 1.56–1.23 (*m*, 18 H, $-CH_2$), 0.94 (*m*, 9 H, $-CH_3$). ^{13}C NMR (DMSO, 100 MHz, δ/ppm): 151.1, 151.0, 150.9, 150.1, 148.2, 140.7, 133.7, 132.6, 132.0, 131.6, 124.2, 113.9, 113.4, 31.7, 31.5, 30.0, 28.7, 22.5, 14.3. MALDI-TOF MS ($C_{58}H_{57}N_5O_2S_4Zn$) *m*/*z*: calcd for 1047.26; found 1047.49.

*2.4.5. 5-(Thien-2-yl)-10,15,20-tris(5-methylthien-2-yl)porphyrin (**2-b**)*

The synthetic procedure for **2-b** was similar to that for **1-b**, except that **2-a** (6.3 g, 50 mmol) was used instead of **1-a**. A purple solid of compound **2-b** was obtained (1.3 g, 11.4%). ^{1}H NMR ($CDCl_3$, 400 MHz, δ/ppm): 9.10–9.02 (*m*, 8 H, pyrrolic-H), 7.92 (*d*, 1 H, Th–H), 7.86–7.85 (*d*, 1 H, Th–H), 7.68–7.67 (*d*, 3 H, Th–H), 7.51–7.50 (*m*, 1 H, Th–H), 7.16 (*d*, 3 H, Th–H), 2.82 (*s*, 9 H, $-CH_3$), −2.61 (*s*, 2 H, −NH). ^{13}C NMR ($CDCl_3$, 100 MHz, δ/ppm): 142.6, 133.8, 133.0, 127.8, 126.0, 124.6, 15.5. MALDI–TOF MS ($C_{39}H_{28}N_4S_4$) *m*/*z* : calcd for 681.12; found 681.18.

2.4.6. 5-(5-Formylthien-2-yl)-10,15,20-tris(5-methylthien-2-yl) porphyrin (2-c)

The synthetic procedure for **2-c** was similar to that for **1-c**, except that **2-b** (0.50 g, 0.74 mmol) was used instead of **1-b**. A purple solid of compound **2-c** was obtained (0.21 g, 40.1%). ^{1}H NMR ($CDCl_3$, 400 MHz, δ/ppm): 10.24 (s, 1 H, −CHO), 9.12–8.98 (*m*, 8 H, pyrrolic-H), 8.16 (*d*, 1 H, Th–H), 8.00 (*d*, 1 H, Th–H), 7.69 (*d*, 3 H, Th–H), 7.17 (*d*, 3 H, Th–H), 2.83 (*s*, 9 H, $-CH_3$), −2.61 (*s*, 2 H, −NH). ^{13}C NMR ($CDCl_3$, 100 MHz, δ/ppm): 183.4, 153.3, 145.6, 142.7, 140.0, 134.8, 134.0, 124.4, 113.6, 113.3, 109.7, 15.5. MALDI–TOF MS ($C_{40}H_{28}N_4OS_4$) *m*/*z* : calcd for 709.15; found 709.24.

2.4.7. 5-(5-Formylthien-2-yl)-10,15,20-tris(5-methylthien-2-yl) porphyrin zine (2-d)

The synthetic procedure for **2-d** was similar to that for **1-d**, except that **2-c** (0.2 g, 0.28 mmol) was used instead of **1-c**. A purple solid of compound **2-d** was obtained (0.21 g, 97%). ^{1}H NMR ($CDCl_3$, 400 MHz, δ/ppm): 10.24 (*s*, 1 H, −CHO), 9.12–8.99 (*m*, 8 H, pyrrolic-H), 8.15 (*d*, 1 H, Th–H), 8.01 (*d*, 1 H, Th–H), 7.69 (*d*, 3 H, Th–H), 7.17 (*d*, 3 H, Th–H), 2.83 (*s*, 9 H, $-CH_3$). MALDI–TOF MS ($C_{40}H_{26}N_4OS_4Zn$) *m*/*z* : calcd for 771.02; found 771.09.

2.4.8. 2-Cyano-3-(5-(10,15,20-tris(5-methylthien-2-yl)) porphyrinatozinc(II)yl)thienyl acrylic acid (Z2)

The synthetic procedure for **Z2** was similar to that for **Z1**, except that **2-d** (0.20 g, 0.26 mmol) was used instead of **1-d**. A purple solid of compound **Z2** was obtained (0.08 g, 36.9%). FT-IR (KBr, ν_{max}/cm^{-1}): 2880, 2843, 2852, 2356, 2217, 1623, 1456, 1384, 996, 1071, 798, 668. UV–vis λ_{max} ($CHCl_3$)/nm: 431, 560. ^{1}H NMR (DMSO, 400 MHz, δ/ppm): 9.07 (*m*, 8 H, pyrrolic-H), 8.61 (*s*, 1 H, vinyl-H), 8.31 (*s*, 1 H, Th–H), 8.12 (*s*, 1 H, Th–H), 7.73 (*s*, 3 H, Th–H),7.27 (*s*, 3H, Th–H), 2.79 (*s*, 9 H, $-CH_3$). ^{13}C NMR (DMSO, 100 MHz, δ/ppm): 151.1, 151.0, 150.9, 150.3, 142.2, 141.0, 134.6, 133.9, 132.5, 132.2, 131.8, 125.4, 113.4, 15.6. MALDI–TOF MS ($C_{43}H_{27}N_5O_2S_4Zn$) *m*/*z* : calcd for 837.15; found 837.03.

2.4.9. 3-Hexylthiophene-2-carbaldehyde (3-a)

Dried magnesium pieces (0.4 g, 17 mmol) were placed into a dry 100 mL three-necked round-bottomed flask together with a few small crystals of iodine. THF (10 mL) was added sequentially under Ar atmosphere, and then a THF solution of 2-bromo-3-hexylthiophene (4.41 g, 15 mmol) was dropped slowly at 60–70 °C. After 6 h, the reaction mixture was cooled down to −40 °C and 6 mL DMF was added. The reaction was allowed to progress for a further 20 h after warming to room temperature. At last, 10 mL diluent hydrochloric acid was added into it. The solution was extracted with dichloromethane, and washed with H_2O. The organic layer was dried over anhydrous $MgSO_4$. Solvent was removed by rotary evaporation, and the residue was purified by silica gel column chromatography with petroleum ether/dichloromethane (5/1) as eluent to yield **3-a** as a buff liquid (1.5 g, 50%). ^{1}H NMR ($CDCl_3$, 400 MHz, δ/ppm): 10.05 (*s*, 1 H, −CHO), 7.66–7.64 (*d*, 1 H, Th−H), 7.02–7.01 (*d*, 1 H, Th−H), 2.99–2.96 (*t*, 2 H, $-CH_2$), 1.71–1.64 (*m*, 4 H, $-CH_2$), 1.38–1.27 (*m*, 4 H, $-CH_2$), 0.91–0.88 (*t*, 3 H, $-CH_3$). ^{13}C NMR ($CDCl_3$, 100 MHz, δ/ppm): 182.1, 152.7, 137.7, 134.3, 130.6, 31.5, 31.3, 28.9, 28.5, 22.5, 13.9.

2.4.10. 5-(3-Hexylthien-2-yl)-10,15,20-tris(5-methylthien-2-yl) porphyrin (3-b)

The synthetic procedure for **3-b** was similar to that for **2-b**, except that **3-a** (1.88 g, 17 mmol) was used instead of 2-thiophenealdehyde. A purple solid of compound **3-b** was obtained (1.0 g, 7%). ^{1}H NMR ($CDCl_3$, 400 MHz, δ/ppm): 9.12–8.90 (*m*, 8 H, pyrrolic-H), 7.75–7.74 (*t*, 1 H, Th−H), 7.69 (*d*, 3 H, Th−H), 7.39–7.37 (*t*, 1 H, Th−H), 7.17 (*s*, 3 H, Th−H), 2.84–2.75 (*s*, 9 H, $-CH_3$), 2.49–2.45(*t*, 2 H, $-CH_2$), 1.45 (*t*, 2 H, $-CH_2$), 1.28 (*t*, 2 H, $-CH_2$), 0.94–0.81 (*m*, 4 H, $-CH_2$), 0.54–0.51 (*t*, 3 H, $-CH_3$), −2.60 (*s*, 2 H, −NH). ^{13}C NMR ($CDCl_3$, 100 MHz, δ/ppm): 145.8, 142.5, 140.2, 133.8, 133.7, 127.2, 125.6, 124.5, 113.0, 112.7, 111.1, 31.2, 30.3, 29.3, 28.7, 22.7, 22.2, 14.1. MALDI-TOF MS ($C_{45}H_{40}N_4S_4$) *m*/*z*: calcd for 765.21; found 765.30.

2.4.11. 5-(3-Hexyl-5-formylthien-2-yl)-10,15,20-tris (5-methylthien-2-yl)porphyrin (3-c)

The synthetic procedure for **3-c** was similar to that for **1-c**, except that **3-b** (0.5 g, 0.58 mmol) was used instead of **2-b**. A purple solid of compound **3-c** was obtained (0.21 g, 40.7%). ^{1}H NMR ($CDCl_3$, 400 MHz, δ/ppm): 10.21 (*s*, 1 H, −CHO), 9.11–8.80 (*m*, 8 H, pyrrolic-H), 8.06 (*d*, 1 H, Th−H), 7.68 (*d*, 3 H, Th−H), 7.16 (*d*, 3 H, Th−H), 2.82 (*s*, 9 H, $-CH_3$) 2.45–2.42 (*t*, 2 H, $-CH_2$), 1.45–1.42 (*m*, 2 H, $-CH_2$), 1.25 (*m*, 2 H, $-CH_2$), 0.92–0.80 (*m*, 4 H, $-CH_2$), 0.52–0.49 (*m*, 3 H, $-CH_3$), −2.61 (*s*, 2 H, −NH). ^{13}C NMR ($CDCl_3$, 100 MHz, δ/ppm): 183.2, 148.0, 147.5, 143.3, 142.7, 140.2, 140.0, 136.0, 133.9, 124.6, 113.8, 113.2, 108.8, 31.1, 30.0, 29.7, 28.6, 22.2, 21.5, 15.5, 13.7. MALDI−TOF MS ($C_{46}H_{40}N_4OS_4$) *m*/*z*: calcd for 793.20; found 793.28.

2.4.12. 5-(3-Hexyl-5-formylthien-2-yl)-10,15,20-tris(5-methylthien-2-yl)porphyrin zine (3-d)

The synthetic procedure for **3-d** was similar to that for **1-d**, except that **3-c** (0.21 g, 0.24 mmol) was used instead of **1-c**. A purple solid of compound **3-d** was obtained (0.20 g, 90%). ^{1}H NMR ($CDCl_3$, 400 MHz, δ/ppm): 10.21 (*s*, 1 H, −CHO), 9.11–8.83 (*m*, 8 H, pyrrolic-H), 8.07 (*d*, 1 H, Th−H), 7.67 (*d*, 3 H, Th−H), 7.16 (*d*, 3 H, Th−H), 2.82(*s*, 9 H, $-CH_3$) 2.45–2.42(*t*, 2 H, $-CH_2$), 1.45–1.42 (*m*, 2 H, $-CH_2$), 1.25 (*m*, 2 H, $-CH_2$), 0.92–0.80 (*m*, 4 H, $-CH_2$), 0.52–0.49 (*m*, 3 H, $-CH_3$). MALDI−TOF MS ($C_{46}H_{38}N_4OS_4Zn$) *m*/*z*: calcd for 855.15; found 855.21.

2.4.13. 2-Cyano-3-(4-hexyl-5-(10,15,20-tris(5-methylthien-2-yl)) porphyrinatozinc(II)yl)thienyl acrylic acid (Z3)

The synthetic procedure for **Z3** was similar to that for **Z1**, except that **3-d** (0.20 g, 0.21 mmol) was used instead of **1-d**. A purple solid of compound **Z3** was obtained (0.08 g, 26%). FT-IR (KBr, ν_{max}/cm^{-1}): 2959, 2927, 2851, 2347, 2216, 1622, 1449, 1384, 1068, 979, 793, 784. UV−vis λ_{max} ($CHCl_3$)/nm: 432, 558. ^{1}H NMR ($CDCl_3$, 400 MHz, δ/ppm): 9.25–8.93 (*m*, 8 H, pyrrolic-H), 8.60 (*s*, 1 H, vinyl-H), 8.21 (*s*, 1 H, Th−H), 7.70–7.69 (*s*, 3 H, Th−H), 7.17 (*s*, 3 H, Th−H), 2.84 (*s*, 9 H, $-CH_3$), 2.52–2.49 (*t*, 2 H, $-CH_2$), 1.47–1.27 (*m*, 4 H, $-CH_2$), 0.93–0.80 (*m*, 4 H, $-CH_2$), 0.51–0.47 (*t*, 3 H, $-CH_3$). ^{13}C NMR (DMSO, 100 MHz, δ/ppm): 151.1, 150.9, 150.8, 150.5, 145.9, 142.1, 142.1, 141.0, 140.9, 133.8, 133.2, 131.6, 132.3, 132.2, 132.1, 131.5, 130.5, 125.3, 125.0, 123.6, 113.7, 113.3, 110.0, 29.7, 29.3, 28.9, 28.3, 22.0, 20.8, 15.5, 13.9. MALDI−TOF MS ($C_{49}H_{39}N_5O_2S_4Zn$) *m*/*z* : calcd for 921.12; found 921.23.

2.4.14. 5-(3,4-Ethylenedioxyl)thienyl-10,15,20-tris(5-methylthien-2-yl)porphyrin (4-b)

The synthetic procedure for **4-b** was similar to that for **1-b**, except that **4-a** (2.88 g, 17 mmol) was used instead of 2-thiophenealdehyde. A purple solid of compound **4-b** was obtained (1.2 g, 9.6%). ^{1}H NMR ($CDCl_3$, 400 MHz, δ/ppm): 9.15–9.11 (*m*, 8 H, pyrrolic-H), 7.69–7.68 (*d*, 3 H, Th−H), 7.17 (*d*, 3 H, Th−H), 6.93 (*s*, 1 H, Th−H), 4.45 (*t*, 2 H, $-OCH_2$), 4.28 (*t*, 2 H, $-OCH_2$), 2.84 (*s*, 9 H, $-CH_3$), −2.58 (*s*, 2 H, −NH). ^{13}C NMR ($CDCl_3$, 100 MHz, δ/ppm): 142.5, 140.5, 140.3, 133.8, 133.7, 131.0, 129.0, 128.2, 125.3, 124.5, 117.0, 113.2, 112.7, 108.7, 101.3, 64.8, 15.5. MALDI-TOF MS ($C_{41}H_{30}N_4O_2S_4$) *m*/*z*: calcd for 739.12; found 739.19.

2.4.15. 5-[5-(3,4-Ethylenedioxyl-5-formyl)thienyl-10,15,20-tris(5-methylthien-2-yl) porphyrin (4-c)

The synthetic procedure for **4-c** was similar to that for **1-c**, except that **4-b** (0.60 g, 0.81 mmol) was used instead of **2-b**. A purple solid of compound **4-c** was obtained (0.30 g, 48.3%). ^{1}H NMR ($CDCl_3$, 400 MHz, δ/ppm): 10.30 (*s*, 1 H, −CHO), 9.16–9.05 (*m*, 8 H, pyrrolic-H), 7.70 (*d*, 3 H, Th−H), 7.17 (*d*, 3 H, Th−H), 4.60 (*t*, 2 H, $-OCH_2$), 4.33 (*t*, 2 H, $-OCH_2$), 2.84 (*s*, 9 H, $-CH_3$), −2.60 (*s*, 2 H, −NH). ^{13}C NMR ($CDCl_3$, 100 MHz, δ/ppm): 180.0, 147.2, 142.7, 140.1, 140.0, 133.9, 128.5, 124.6, 119.6, 114.0, 113.2, 106.2, 65.5, 64.6, 15.5. MALDI-TOF MS ($C_{42}H_{30}N_4O_3S_4$) *m*/*z*: calcd for 767.12; found 767.26.

2.4.16. 5-[5-(3,4-Ethylenedioxyl-5-formyl)thienyl-10,15,20-tris(5-methylthien-2-yl) porphyrin zine (4-d)

The synthetic procedure for **4-d** was similar to that for **1-d**, except that **4-c** (0.3 g, 0.39 mmol) was used instead of **1-c**. A purple solid of compound **4-d** was obtained (0.31 g, 95%). ^{1}H NMR ($CDCl_3$, 400 MHz, δ/ppm): 10.31 (*s*, 1 H, −CHO), 9.15–9.02 (*m*, 8 H, pyrrolic-H), 7.71 (*d*, 3 H, Th−H), 7.17 (*d*, 3 H, Th−H), 4.60 (*t*, 2 H, $-OCH_2$), 4.33 (*t*, 2 H, $-OCH_2$), 2.84 (*s*, 9 H, $-CH_3$). MALDI−TOF MS ($C_{42}H_{28}N_4O_3S_4Zn$) *m*/*z*: calcd for 829.05; found 829.11.

2.4.17. 2-Cyano-3-(3,4-ethylenedioxyl-5-(10,15,20-tris(5-methylthien-2-yl)) porphyrinatozinc(II)yl)thienyl acrylic acid (Z4)

The synthetic procedure for **Z4** was similar to that for **Z1**, except that **4-d** (0.20 g, 0.24 mmol) was used instead of **1-d**. A purple solid of compound **Z4** was obtained (0.12 g, 56.1%). FT-IR (KBr, ν_{max}/cm^{-1}): 2966, 2843, 2364, 2206, 1611, 1579, 1441, 1383, 1319, 1261, 1015, 1071, 799, 712. UV−vis λ_{max} ($CHCl_3$)/nm: 435, 562. ^{1}H NMR (DMSO, 400 MHz, δ/ppm): 9.16–9.06 (*m*, 8 H, pyrrolic-H), 8.51 (*s*, 1 H, vinyl-H), 7.72 (*d*, 3 H, Th−H), 7.27 (*d*, 3 H, Th−H), 4.65 (*t*, 2 H, $-OCH_2$). 4.37 (*t*, 2 H, $-OCH_2$), 2.78 (*s*, 9 H, $-CH_3$). ^{13}C NMR (DMSO, 100 MHz, δ/ppm): 151.1, 150.9, 150.8, 150.4, 142.2, 141.0, 133.9, 132.3, 132.1, 131.9, 125.4, 113.3, 22.9, 15.5. MALDI−TOF MS ($C_{45}H_{29}N_5O_4S_4Zn$) *m*/*z*: calcd for 895.04; found 895.12.

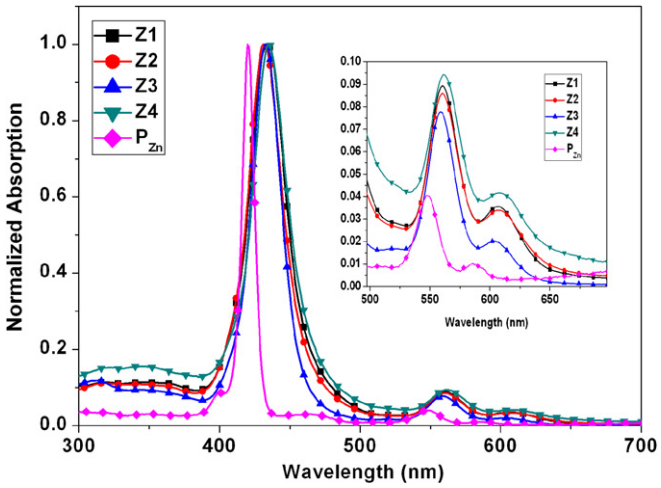

Fig. 3. Normalized absorption spectra of the porphyrin dyes in $CHCl_3$. The inset is an expansion of the Q-band region.

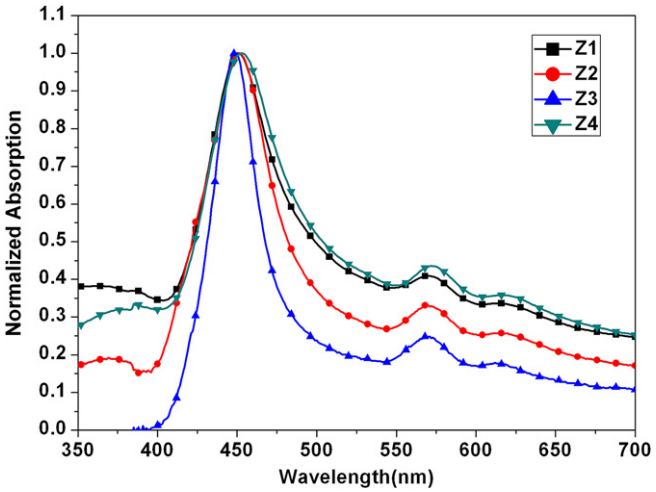

Fig. 4. UV–visible absorption spectra of the porphyrin dyes adsorbed on TiO_2 films.

3. Results and discussion

3.1. Synthesis

The detailed synthetic routes of four porphyrin dyes as well as the intermediates are shown in Fig. 2. Functionalized porphyrins as donors in this study were synthesized by the Adler–Longo method [12]. Taking **Z1** as an example, the dye was synthesized as the following steps. First, 5-hexylthiophene-2-aldehyde **1-a,** was obtained from 2-hexylthiophene by Vilsmeier formylation with $POCl_3$ and DMF in 1,2-dichloroethane. Then compound **1-a** was reacted with 2-thiophenealdehyde and pyrrole by the Adler–Longo method to obtain crude compound. After reduced pressure distillation, recrystallization and purification twice by column chromatography on silica gel, the key intermediate **1-b** was achieved. Subsequently, compound **1-b** was reacted with $POCl_3$ and DMF in 1,2-dichloroethane via Vilsmeier formylation to convert to **1-c**. Finally, compound **1-c** was treated with $Zn(OAc)_2$ to obtain **1-d** and then reacted with cyanoacetic acid by Knoevenagel reaction to give the target dye **Z1**. **Z2**, **Z3** and **Z4** were synthesized by the similar procedure. It is noted that compound **3-a** was synthesized by Grignard reaction with 2-bromo-3-hexylthiophene as the starting material. The structures of the four dyes were verified by FT-IR, ^1H NMR, ^{13}C NMR and MALDI–TOF mass spectra.

3.2. Optical properties

The UV–visible absorption spectra of **Z1**–**Z4** and $\mathbf{P_{Zn}}$ [18] in the $CHCl_3$ solution are displayed in Fig. 3, and the corresponding data are collected in Table 1. Owing to their similar structures, all the porphyrin dyes exhibit the strong absorption peaks located in the range of 400–440 nm (Soret-band) and weak Q-bands around 560 nm which are attributed to π–π^* electron transition. The values of the molar extinction coefficient (ε) at the maximum absorption wavelength (λ_{max}) for the **Z**-series of dyes are in the range of 0.86–2.59 $\times$ 10^5 dm^3 mol^{-1} cm^{-1}. As expected, the UV–visible absorption bands of the four dyes are sensitive to substituents on the periphery of the porphyrin ring respectively. All of the Soret-bands of **Z1**–**4** are red-shifted and broadened significantly relative to the reference porphyrin $\mathbf{P_{Zn}}$ [18], and the Q-bands are red-shifted and broadened evidently in the expansion. The maximum absorption wavelength (λ_{max}) for these dyes are 434, 431, 433 and 435 nm, respectively. And all the Soret-bands of the four dyes are 9–13 nm red-shifted than the porphyrins which contain alkylphenyl units at the *meso*-position [18,19]. The increase in red-shift of the absorption band is possibly due to the electronic effect of the thienyl groups [11]. This result conforms that the alkylthienyls appending on porphyrin cycles have positive effect on improving the UV–visible absorption of the porphyrin dyes. The molar extinction coefficient (ε) of **Z4** is smaller than three dyes (**Z1**–**3**) indicating the inferior ability of light harvesting. We also

Table 1
UV–visible, PL spectral data of the porphyrin dyes.

Dye	Soret/Q-band(s)[a] (ε, 10^5 M^{-1} cm^{-1})[a]	Soret/Q-band (f)[b]	Γ[c]/10^{-8} mol cm^{-2}	λ_{em} (nm)[d]	λ_{int} (nm)[e]
Z1	434 (2.57), 560 (0.23)	451/560	2.90	695	593
Z2	431 (1.93), 560 (0.17)	452/561	4.84	692	590
Z3	433 (1.63), 558 (0.13)	450/559	3.83	656	580
Z4	435 (0.86), 559 (0.07)	452/573	4.27	641	593
$\mathbf{P_{Zn}}$	420 (2.21), 547 (0.07)	–	–	598, 645	448

[a] Absorption spectra was measured in $CHCl_3$ solution.
[b] Absorption spectra was obtained on TiO_2 films.
[c] Amount of the dyes adsorbed on TiO_2 films.
[d] Wavelengths for emission spectra in $CHCl_3$ solution by exciting at Soret wavelength.
[e] Measured by the intercept of the normalized absorption and emission spectra.

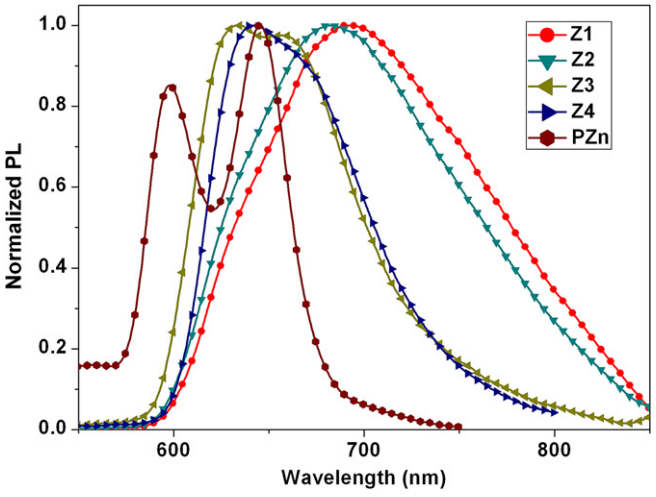

Fig. 5. PL spectra of the porphyrin dyes in $CHCl_3$.

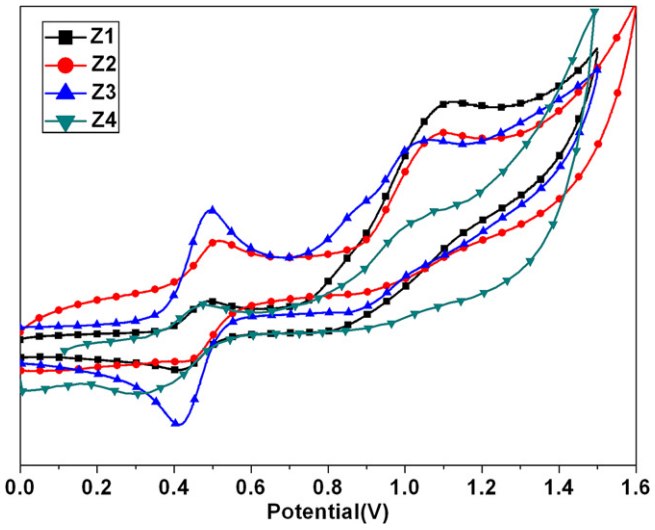

Fig. 6. Cyclic voltammograms of the porphyrin dyes.

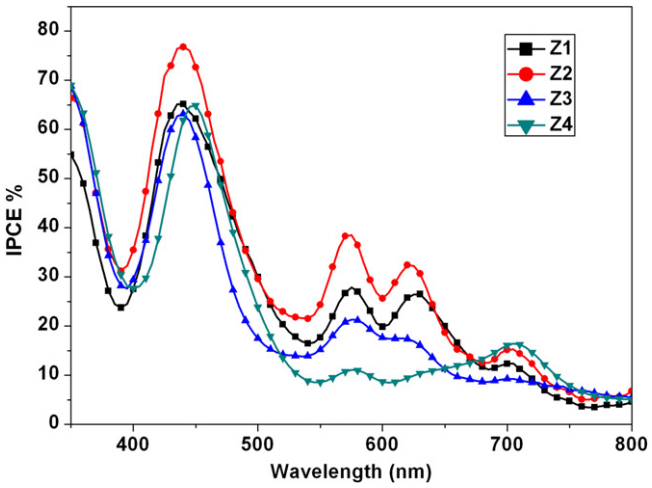

Fig. 7. IPCE plots for the DSSCs based on the porphyrin dyes.

measured the adsorption of the four porphyrin dyes on TiO_2 films on quartz plate (Fig. 4) to obtain red-shifted and broadened spectra in comparison with those of the solution spectra, which should result from the formation of the *J*-type aggregate of porphyrins on the TiO_2 surface [14].

The emission spectra of these porphyrin dyes are presented in Fig. 5 and fluorescence data are also listed in Table 1. The maximum fluorescence emission wavelength (λ_{em}) of **Z1** and **Z2** are 695 and 692 nm, respectively, which are red-shifted relative to **Z3** (656 nm) and **Z4** (641 nm). The observed red-shifts of λ_{em} should be attributed to the increase of the effective conjugation in **Z1** and **Z2** molecules compared to **Z3** and **Z4**. This can be explained by the fact that there are much bigger dihedral angles between the prophyrin core and the π-bridge due to the substituents for **Z3** and **Z4**, which lower the π-conjugation [20] of the D-π-A system thus resulting in the ineffective intramolecular electron transfer.

3.3. Electrochemical properties

The electrochemical studies are performed on the four dyes to elucidate the effect of thienyl groups on the energy level of the porphyrin macro-cycle. The reduction potentials were determined by differential pulse voltammetry (DPV) and the oxidation potentials (E_{ox}) corresponding to the HOMO (highest occupied molecular orbital) energy levels of the porphyrin dyes were determined via cyclic voltammetry (Fig. 6). All the data are summarized in Table 2, which are consistent with previous reports [11]. The reduction potentials of the four dyes (**Z1**–**4**) are −1.104, −1.216, −1.176 and −1.124 eV, respectively, which are positive than $\mathbf{P_{Zn}}$ (−1.290 eV). E_{ox} is the first oxidation potentials (*vs.* NHE), and E_{0-0} is determined from the intercept of the normalized absorption and emission spectra. Then we consider the potential levels of (E_{ox}–E_{0-0}) corresponding to the LUMO (lowest unoccupied molecular orbital) level of the dyes. By the introduction of thienylgroups at the *meso*-positions of porphyrin dyes, the energy level of LUMO is significantly shifted to the positive compared with the reference $\mathbf{P_{Zn}}$ [18] and the HOMO energy levels are negatively shifted, indicating a decreased HOMO–LUMO energy gap. Furthermore, for dyes **Z1**–**Z4** with the introduction of electron-donating groups into the porphyrin ring, a decrease of the HOMO–LUMO energy gaps relative to $\mathbf{P_{Zn}}$ is observed, which is consistent with the red-shift in the absorption and emission spectra. As shown in Table 2, the sufficiently low HOMO energy level of the dye will ensure that there is enough driving force for the dye regeneration reaction to compete efficiently with the recapture of the injected electrons by the dye cation radical. While the LUMO energy level is more negative than the conduction band (CB) of TiO_2 (−0.5 V *vs.* NHE) [21,22], indicating sufficient driving force for electron transfer from the excited dye molecules to the conduction band of TiO_2 electrode.

Table 2
Electrochemical data for the porphyrin dyes and driving forces for electron transfer processes on the TiO_2.

Dye	E_{0-0}[a] (eV)	E_{ox}[b] (V)	E_{red}[c] (V)	E_{ox}*[d] (V)	ΔG_{inj}[e](eV)	ΔG_{reg}[f](eV)
Z1	2.091	1.220	−1.104	−0.871	−0.371	−0.720
Z2	2.102	1.207	−1.216	−0.895	−0.395	−0.707
Z3	2.126	1.161	−1.176	−0.977	−0.477	−0.661
Z4	2.091	1.167	−1.124	−0.924	−0.424	−0.667
$\mathbf{P_{Zn}}$	2.77	1.230	−1.290	−1.540	−1.040	−0.730

[a] Determined from the intercept of the normalized absorption and emission spectra.
[b] First oxidation potentials (*vs.* NHE).
[c] First reduction potentials (*vs.* NHE).
[d] Excited-state oxidation potentials approximated from E_{ox} and E_{0-0} (*vs.* NHE).
[e] Driving forces for electron injection from the porphyrin excited singlet state (E_{ox}*) to the conduction band of TiO_2 (−0.5 V *vs.* NHE).
[f] Driving forces for regeneration of the porphyrin radical cation by I^-/I_3^- redox couple (+0.5 V *vs.* NHE).

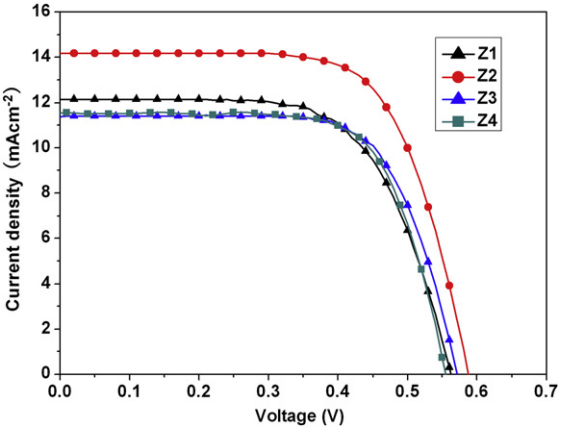

Fig. 8. Current–voltage characteristics of the porphyrin dyes.

Table 3
Photovoltaic performances of DSSCs based on the porphyrin dyes.

Dye	J_{sc} (mA/cm^2)	V_{oc} (V)	ff	η (%)
Z1	12.13 ± 0.10	0.56 ± 0.01	0.65 ± 0.01	4.44 ± 0.10
Z2	14.18 ± 0.13	0.59 ± 0.01	0.68 ± 0.01	5.71 ± 0.05
Z3	11.37 ± 0.18	0.57 ± 0.01	0.70 ± 0.01	4.54 ± 0.05
Z4	11.56 ± 0.18	0.56 ± 0.01	0.70 ± 0.02	4.54 ± 0.10

3.4. Photovoltaic properties of porphyrin-sensitized TiO_2 cells

The incident photo-to-current conversion efficiencies (IPCE) plots for the DSSCs based on the four porphyrin dyes are shown in Fig. 7. The four dyes all respond in the broad rang of 350–800 nm and show the maximum IPCE values around 450 nm, which is in accord with the spectra of the dyes in solid films. Among the four dyes, **Z2** exhibits the highest IPCE (~78%) due to its largest adsorbed amounts of the dye on the TiO_2 film and relatively better ability of light harvesting, which implies this sensitizer would show a relatively large photocurrent in DSSCs. On the other hand, **Z4** shows inferior IPCE in the range of 550–650 nm relative to other three dyes which mainly resulted from the smaller Γ value and worse ability of light harvesting.

The photovoltaic characteristics of DSSCs based on the four dyes are shown in Fig. 8 and the device performance parameters are listed in Table 3. The open-circuit photovoltage (V_{oc}) values are in the order of **Z2** > **Z3** > **Z1** ≈ **Z4**, and the short-circuit photocurrent density (J_{sc}) are **Z2** > **Z1** > **Z3** ≈ **Z4**. The measured results of V_{oc} values are consistent with the discussion of their electrochemical properties. To investigate the absorptive abilities and explain the J_{sc} of the Z-series of dyes the thin films were evaluated for the total amount of the porphyrin adsorbed. The adsorbed amounts (Γ) of the four dyes are exhibited in Table 1. The adsorbed amounts of four dyes are 2.90×10^{-8}, 4.84×10^{-8}, 3.83×10^{-8}, and 4.27×10^{-8} mol/cm^2 for **Z1**, **Z2**, **Z3**, and **Z4**, respectively. The Γ is in the order of **Z2** > **Z4** > **Z3** > **Z1**. Because Γ is related to the molecular size and the thickness of dye aggregates [23], which correlates directly to the absorptive abilities of the four dyes and may influence the photovoltaic performance of solar cells. For **Z1**, the *n*-hexyl substituents around the porphyrin core sterically hinder adsorption. In detail, **Z3** features a long alkyl chain on the thiophene bridge between the porphyrin core and the anchor group resulted in a much bigger dihedral angle of the porphyrin to reduce the coplanarity of the donor and the acceptor unit. And in the unit of **Z4**, the EDOT (3,4-ethylenedioxythienyl) segment is larger than the thienyl segment leading to a more twisted nonplanar geometry. Finally, due to the smallest molecular size, **Z2** is prone to be the largest Γ and result in the highest J_{sc}, which is in agreement with the IPCE. The DSSCs based on **Z3** and **Z4** show the same η (4.54%) because of their almost identical V_{oc} and J_{sc} values. Summarily, **Z2** obtains the best IPCE, the hightest V_{oc} value (0.59 V) and J_{sc} value (14.18 mA/cm^2), and the best η of 5.71%.

4. Conclusions

In conclusion, four porphyrin dyes (**Z1**–**Z4**) with thienyl appended porphyrins as electron donors, thiophene derivatives as linkers and 2-cyanoacrylic acids as anchor groups were designed, synthesized and characterized for DSSCs to obtain the highest η up to 5.71%. The appended alkylthienyl units and various thiophene linkers significantly influence the photophysical, electrochemical and photovoltaic properties of the four dyes. With the introduction of these alkylthienyl units around the porphyrin cycles, the absorption spectra were red-shifted and broadened and the HOMO–LUMO energy gaps were decreased as expected. To utilize more solar light, we should further design and synthesis new porphyrin dyes which have broadened spectra between the Soret-bands, the Q-bands and/or intensify the Q-bands as much as they can.

Acknowledgments

This work was supported by the National Natural Science Foundation of China (50973092, 51003089), Specialized Research Fund for the Doctoral Program of Higher Education of China (20094301120005, 20104301110003), and Natural Science Foundation (09JJ3020, 09JJ4005) of Hunan Province of China.

References

[1] Robertson N. Optimizing dyes for dye-sensitized solar cells. Angewandte Chemie International Edition 2006;45:2338–45.
[2] O'Regan B, Grätzel M. A low-cost high-efficiency solar cell based on dye-sensitized colloidal TiO_2 film. Nature 1991;353:737–9.
[3] Mishra A, Fischer MKR, Bäerle P. Metal-free organic dyes for dye-sensitized solar cells: from structure: property relationships to design rules. Angewandte Chemie International Edition 2009;48:2474–99.
[4] Imahori H, Umeyama T, Ito S. Large π-aromatic molecules as potential sensitizers for highly efficient dye-sensitized solar cells. Accounts of Chemical Research 2009;42(11):1809–18.
[5] (a) Nazeeruddin MK, Angelis DF, Fantacci S, Selloni A, Viscardi G, Liska P, et al. Combined experimental and DFT-TDDFT computational study of photoelectrochemical cell ruthenium sensitizers. Journal of the American Chemical Society 2005;127:16835–47;
(b) Wang P, Klein C, Moser JE, Baker RH, Ha NLC, Charvet R, et al. Amphiphilic ruthenium sensitizer with 4,40-diphosphonic acid-2,20-bipyridine as anchoring ligand for nanocrystalline dye sensitized solar cells. Journal of Physical Chemistry B 2004;108:17553–9.
[6] Calogero G, Marco GD, Caramori S, Cazzanti S, Argazzi R, Bignozzi CA. Natural dye senstizers for photoelectrochemical cells. Energy & Environmental Science 2009;2:1162–72.
[7] Eu S, Hayashi S, Umeyama T, Matano Y, Araki Y, Imahori H. Quinoxaline-fused porphyrins for dye-sensitized solar cells. Journal of Physical Chemistry C 2008;112:4396–405.
[8] Liao MS, Scheiner S. Electronic structure and bonding in metal porphyrins, metal=Fe, Co, Ni, Cu, Zn. Journal of Chemical Physics 2002;117:205–19.
[9] Campbell WM, Jolley KW, Wagner P, Wagner K, Walsh PJ, Gordon KC, et al. Highly efficient porphyrin sensitizers for dye-sensitized solar cells. Journal of Physical Chemistry C 2007;111:11760–2.
[10] (a) Hsieh CP, Lu HP, Chiu CL, Lee CW, Chuang SH, Mai CL, et al. Synthesis and characterization of porphyrin sensitizers with various electron-donating substituents for highly efficient dye-sensitized solar cells. Journal of Materials Chemistry 2010;20:1127–34;
(b) Lu HP, Tsai CY, Yen WN, Hsieh CP, Lee CW, Yeh CY, et al. Control of dye aggregation and electron injection for highly efficient porphyrin sensitizers adsorbed on semiconductor films with varying ratios of coadsorbate. Journal of Physical Chemistry C 2009;113:20990–7;
(c) Bessho T, Zakeeruddin SM, Yeh CY, Diau EWG, Grätzel M. Highly efficient mesoscopic dye-sensitized solar cells based on donor–acceptor-substituted porphyrins. Angewandte Chemie International Edition 2010;49:6646–9;
(d) Imahori H, Matsubara Y, Iijima H, Umeyama T, Matano Y, Ito S, et al. Effects of *meso*-diarylamino group of porphyrins as sensitizers in dye-Sensitized solar cells on optical, electrochemical, and photovoltaicproperties. Journal of Physical Chemistry C 2010;114:10656–65.
[11] Bhyrappa P, Bhavana P. Meso-tetrathienylporphyrins: electrochemical and axial ligation properties. Chemical Physical Letters 2001;349:399–404.
[12] Boylea NM, Rochfordb J, Prycea MT. Thienyl-appended porphyrins: synthesis, photophysical and electrochemical properties, and their applications. Coordination Chemistry Reviews 2010;254:77–102.
[13] Ziessel R, Bäuerle P, Ammann M, Barbieri A, Barigelletti F. Exciton-like energy collection in an oligothiophene wire end-capped by Ru- and Os-polypyridine chromophores. Chemical Communication 2005;6:802–5.
[14] Li G, Jiang K, Bao P, Li Y, Li S, Yang L. Molecular design of triarylamine-based organic dyes for efficient dye-sensitized solar cells. New Journal of Chemistry 2009;33:868–76.
[15] Kalyanasundaram K, Grätzel M. Applications of functionalized transition metal complexes in photonic and optoelectronic devices. Coordination Chemistry Reviews 1998;77:347–414.
[16] Kamat PV, Haria M, Hotchandani S. C_{60} cluster as an electron shuttle in a Ru(II)-polypyridyl sensitizer-based photochemical solar cell. Journal of Physical Chemistry B 2004;108:5166–70.
[17] Koumura N, Wang ZS, Mori S, Miyashita M, Suzuki E, Hara K. Alkyl-functionalized organic dyes for efficient molecular photovoltaics. Journal of the American Chemical Society 2006;128:14256–7.

[18] Xiang N, Huang X, Feng X, Liu Y, Zhao B, Deng L, et al. The structural modification of thiophene-linked porphyrin sensitizers for dye-sensitized solar cells. Dyes and Pigments 2011;88:75–83.
[19] Liu Y, Xiang N, Feng X, Shen P, Zhou W, Weng C, et al. Thiophene-linked porphyrin derivatives for dye-sensitized solar cells. Chemical Communication 2009;18:2499–501.
[20] Umeyama T, Takamatsu T, Tezuka N, Matano Y, Araki Y, Wada T, et al. Synthesis and photophysical and photovoltaic properties of porphyrin–furan and thiophene alternating copolymers. Journal of Physical Chemistry C 2009;113:10798–806.
[21] Hagfeldt A, Grätzel M. Light-induced redox reactions in nanocrystalline systems. Chemical Reviews 1995;95(1):49–68.
[22] Hara K, Sato T, Katoh R, Furube A, Ohga Y, Shinpo A, et al. Molecular design of coumarin dyes for efficient dye-sensitized solar cells. Journal of Physical Chemistry B 2003;107(2):597–606.
[23] Wang ZS, Koumura N, Cui Y, Takahashi M, Sekiguchi H, Mori A, et al. Hexylthiophene-functionalized carbazole dyes for efficient molecular photovoltaics: tuning of solar-cell performance by structural modification. Chemistry of Materials 2008;20:3993–4003.